



INTERNATIONAL JOURNAL OF ENGINEERING SCIENCES & RESEARCH TECHNOLOGY

Performance of Biomass Adsorber Column for Competitive Removal Pb(II), Cr(III) and Cd(II) ions from Synthetic Wastewater

Abbas Hamid Sulaymon, Shahlaa Esmail Ebrahim and Mohanad Jasim Mohammed-Ridha

Environmental Engineering Department, College of Engineering, University of Baghdad, Iraq

inas@yahoo.com

Abstract

The adsorption of Pb(II), Cr(III) and Cd(II) onto dead anaerobic biomass (DAB) in single, binary and ternary system was studied using fixed bed adsorber. A general rate multi- component model (GRM) was utilized to predict the fixed bed breakthrough curves for triple-component system. This model considers both external and internal mass transfer resistances as well as axial dispersion with non-linear multi-component isotherm (Langmuir model). The effects of important parameters, such as flow rate, initial concentration and bed height on the behavior of breakthrough curves were studied. The equilibrium isotherm model parameters such as isotherm model constants, pore diffusion coefficients were obtained from the batch experiments. The results showed that the GRM was found suitable for describing the adsorption process of the dynamic behavior of the DAB adsorber column.

Keywords: Adsorption, DAB, Heavy metals, Fixed bed, GRM.

Introduction

Heavy metals are toxic pollutants released into the environment as a result of different activities such as industrial, mining, and agricultural activities (Alkhalifa et al., 2012). Different methods are used for the removal of heavy metals as important contaminants in wastewater. The chemical methods effectively decrease of heavy metals to acceptable levels required a large excess of chemicals, which increase the costs due to the generating of voluminous sludge (Jianlong and Can, 2009). The use of natural biomass as adsorbent will involve the same concept of separation as in adsorption which is termed as biosorption (Lawrence et al., 2010). Biosorbents for the removal of metals mainly come under the following categories: bacteria, fungi, algae, industrial wastes, agricultural wastes and other polysaccharide materials. In general, all types of biomaterials have shown good biosorption capacities towards all types of metal ions. (Vijayaraghavan and Yun, 2008)

Adsorption is a well-established and powerful technique for treating domestic and industrial effluents (Volesky et al., 2004). The capacities of a many biosorbent were found to be much higher than those of other types of adsorbents, much higher than those of activated carbon, natural zeolites and synthetic ion exchange resins (Zubeyde et al., 2009). Sulaymon et

al., (2013) found that the metal biosorption by bacteria can also be influenced by metal speciation in the aqueous phase as well as by the surface properties, such as charge and orientation of the functional groups on the cell surface. The surface chemistry of DAB and the chemical characteristics of adsorbate, such as polarity, ionic nature, functional groups, and solubility, determine the nature of bonding mechanisms as well as the extent and strength of adsorption. A variety of physicochemical mechanisms/forces, such as van der Waals, H-binding, dipole dipole interactions, ion exchange, covalent bonding, cation bridging, and water bridging, can be responsible for the adsorption of inorganic compounds in DAB (Sulaymon and Ebrahim, 2010).

Fixed bed adsorber is a continuous flow operation adsorption process for industrial applications in wastewater treatment (Gupta and Rastogi, 2009). The design of an adsorption column depends on various important parameters such as flow rate, initial concentration and bed height (mass of adsorbent). Understanding of adsorption characteristics, determination of break point time for adsorption operation and effective utilization of the column is possible by carrying out the mathematical modeling of fixed-bed adsorption column. Continuous adsorption

studies are required to collect the experimental data for the design of adsorption column and for subsequent scale-up from pilot plant to industrial scale operation. Past studies mainly focused on analytical approach of solving the dynamics of fixed-bed adsorption column (Hawari and Mulligan, 2006). These models, exclude some of the important physical aspects such as axial dispersion and intra-particle resistances along the bed length and linear isotherm such as: homogenous surface diffusion model described by Lawrence et al., (2010); second-order reversible reaction model and quasi-chemical kinetic model by Ahmed (2006). In the present study, a general multi-component model is used to predict the breakthrough curves of metal ion mixtures in fixed bed column for single, binary and ternary component onto DAB and compare the experimental results with that simulated by numerical solution of model which includes film mass transfer, pore diffusion resistance, axial dispersion and nonlinear isotherm.

Mathematical Modeling and Simulation

In the present study, a mathematical model for the fixed bed column is used by incorporation of important parameter such as external mass transfer resistance, internal mass transfer resistance and nonlinear multi-component isotherm. The proposed model can be extensively used for understanding the dynamics of fixed bed adsorption column for the adsorption of metal ions compounds. To formulate a generalized model for the fixed bed adsorption column, following assumptions are made (Al-Najar, 2009)

- Equilibrium of adsorption is described by the nonlinear multi-component Langmuir isotherm.
- Mass transfer across the boundary layer surrounding the solid particles is characterized by external-film mass transfer coefficient (k_f).
- Intra-particle mass transfer is characterized by pore diffusion coefficient (D_p)
- Macro-porous adsorbent particles are spherical and homogeneous in size and density.
- Compressibility of the mobile phase is negligible.
- Fluid inside particles (macropores) is stagnant, i.e., there is no convective flow inside macropores.

- The adsorption process is isothermal. There is no temperature change during a run.
- The concentration gradients in the radial direction are negligible.
- All mechanisms which contribute to axial mixing are lumped together into a single axial dispersion coefficient.

Based on the assumption of the model, the governing equations for multi-component system can be obtained from differential mass balance of the bulk-fluid phase and the particles phase respectively:

Continuity equation in the bulk-fluid phase

$$-D_{bi} \frac{\partial^2 C_{bi}}{\partial Z^2} + V_i \frac{\partial C_{bi}}{\partial Z} + \frac{\partial C_{bi}}{\partial t} + \frac{3k_{fi}(1-\varepsilon_b)}{\varepsilon_b R_p} [C_{bi} - C_{pi,R=R_p}] = 0$$

(1)

Continuity equation inside the particle phase

$$(1-\varepsilon_p) \frac{\partial C_{pi}^*}{\partial t} + \varepsilon_p \frac{\partial C_{pi}}{\partial t} - \varepsilon_p D_{pi} \left[\frac{1}{R_p^2} \frac{\partial}{\partial R_p} \left(R_p^2 \frac{\partial C_{pi}}{\partial R_p} \right) \right] = 0$$

(2)

Initial and Boundary Conditions

The initial and boundary conditions may be represented by the following equations

Initial Condition ($t = 0$)

$$C_{bi} = C_{bi}(0, Z) = 0 \quad (3)$$

$$C_{pi} = C_{pi}(0, R, Z) = 0 \quad (4)$$

Boundary Conditions

$$Z = 0: \frac{\partial C_{bi}}{\partial Z} = \frac{v}{D_{bi}} (C_{bi} - C_{oi}) \quad (5)$$

$$Z = L: \frac{\partial C_{bi}}{\partial Z} = 0 \quad (6)$$

$$R = 0: \frac{\partial C_{pi}}{\partial R} = 0 \quad (7)$$

$$R = R_p: \frac{\partial C_{pi}}{\partial R} = \frac{k_{fi}}{\varepsilon_p D_{pi}} (C_{bi} - C_{pi,R=R_p}) \quad (8)$$

Dimensionless Groups

Defining the following dimensionless variables

$$c_{bi} = \frac{C_{bi}}{C_{oi}}, c_{pi} = \frac{C_{pi}}{C_{oi}}, c_{pi}^* = \frac{C_{pi}^*}{C_{oi}}, \tau = \frac{vt}{L}, r = \frac{R}{R_p},$$

$$z = \frac{Z}{L}$$

Also, the dimensionless parameters are defining as

$$Pe_i = \frac{vL}{D_{zi}}, \quad Bi_i = \frac{k_{fi}R_p}{\varepsilon_p D_{pi}}, \quad \eta_i = \frac{\varepsilon_p D_{pi} L}{R_p^2 v}$$

$$\zeta_i = \frac{3Bi_i \eta_i (1 - \varepsilon_b)}{\varepsilon_b}$$

The model equations can be transformed into the following dimensionless equations

$$-\frac{1}{Pe_i} \frac{\partial^2 c_{bi}}{\partial z^2} + \frac{\partial c_{bi}}{\partial z} + \frac{\partial c_{bi}}{\partial \tau} + \zeta_i (c_{bi} - c_{pi,r=1}) = 0 \quad (9)$$

$$\frac{\partial}{\partial \tau} \left[(1 - \varepsilon_p) c_{pi}^* + \varepsilon_p c_{pi} \right] - \eta_i \left[\frac{1}{r^2} \frac{\partial}{\partial r} \left(r^2 \frac{\partial c_{pi}}{\partial r} \right) \right] = 0 \quad (10)$$

In these equations, the Peclet number (Pe_i) reflects the ratio of the convection rate to the dispersion rate, while the Biot number (Bi_i) reflects the ratio of the external film mass transfer rate to the intra-particle diffusion rate.

Initial conditions become ($\tau = 0$) (Sulaymon et al., 2012)

$$c_{bi} = c_{bi}(0, z) = 0 \quad (11)$$

$$c_{pi} = c_{pi}(0, r, z) = 0 \quad (12)$$

And boundary conditions become;

$$z = 0: \frac{\partial c_{bi}}{\partial z} = Pe_i (c_{bi} - 1) \quad (13)$$

$$z = 1: \frac{\partial c_{bi}}{\partial z} = 0 \quad (14)$$

$$r = 0: \frac{\partial c_{pi}}{\partial r} = 0 \quad (15)$$

$$r = 1: \frac{\partial c_{pi}}{\partial r} = Bi_i (c_{bi} - c_{pi,r=1}) \quad (16)$$

The concentration c_{pi}^* in eq. (10) is the dimensionless concentration of component i in the solid phase of the particles. It is directly linked to a multi-component isotherm, which is the extended Langmuir model:

$$C_{pi}^* = \frac{q_{mi} \rho_p b_i C_{pi}}{1 + \sum_{j=1}^{N_s} b_j C_{pj}} = \frac{\rho_p a_i C_{pi}}{1 + \sum_{j=1}^{N_s} b_j C_{pj}} \quad (17)$$

And in dimensionless form:

$$c_{pi}^* = \frac{\rho_p a_i c_{pi}}{1 + \sum_{j=1}^{N_s} (b_j C_{oj}) c_{pj}} \quad (18)$$

Because of nonlinear multi-component Langmuir isotherm is considered, finite elements method (Galerkin weighted residual method) is used for the discretization of the bulk-fluid phase partial differential equation and the orthogonal collocation method for the particle phase equation is produced. The ordinary differential equation system with initial values can be readily solved using an ordinary differential equation solver such as the subroutine "ODE15S" of MATLAB V-7.3 which is a variable order solver based on the numerical differentiation formulas.

Experimental Materials and Procedure Adsorbate

1000 mg/l standard stock solution of lead (II), chromium (II) and cadmium (II) were prepared by dissolving $Pb(NO_3)_2$, $Cr(NO_3)_2$ and $Cd(NO_3)_2$ in distilled water. The salts were bought from Iraqi market with specifications listed in Table 1

Table 1 main physicochemical properties of the metals tested

Properties	Lead	Chromium	Cadmium
Formula	Pb(II) from $Pb(NO_3)_2$	Cr(III) from $Cr(NO_3)_3$	Cd(II) from $Cd(NO_3)_2$
Appearance	White crystals	colorless blue-violet crystals	white crystals
Molar mass, g/mole	331.2	238.011	236.42
Standard atomic weight	207.2	51.99	112.41
Solubility in water, g/100 mL	52	81	136
Molecular diffusion, $m^2/s \times 10^{-8}$	4.98	4.22	4.20
Hydrated ion radius (Å)	4.01	4.13	4.26
Crystal radius (Å)	1.19	0.75	0.97
Electronegativity	2.33	1.66	1.69

Charge	2	3	2
Density, g/cm ³	4.53	1.85	3.60
Wavelengths used by AA, nm	283.3	357.9	228.8
Company	BDH (England)	BDH (England)	Fluka (Switzerland)

Adsorbent

Heterogeneous cultures including mostly anaerobic bacteria, yeast, fungi and protozoa of sorbents supplied from Al-Rostomia'a third extension drying bed Baghdad-Iraq. The physical, chemical and biological properties were measured and listed in Table 2. Anaerobic and facultative anaerobic microorganisms (*Aeromonas species*, *E-coli*,

Pseudomonas aeruginosa, *Clostridium*, *Staphylococcus sp* and *Salmonella sp*, *Rhizopusarrhizus*, *Saccharomyces erevisiae*) were found in biomass from the drying bed using API Instrument (Biomerieux, France). Preparation (DAB) using heterogeneous culture of live anaerobic biomass (LAB) was dried at temperature (37-45°C) for 5 days crushed, sieved, washed with distilled water and dried at 70°C for 6 h.

Table 2 physical chemical and biological characteristic of DAB

Biomass		Biological characteristic (live biomass)	
Physical characteristic (dead biomass)		<i>Bacteria</i>	
Particle diameter, mm	0.775	<i>Aeromonas species</i> , CFU/mL	222000
Surface area, m ² /g	94.53 ^(a)	<i>E-coli</i> , CFU/mL	430000
Actual density, kg/m	1741.6	<i>Pseudomonas aeruginosa</i> , CFU/mL	703500
Bulk density, kg/m	609.9 ^(b)	<i>Klebsiella species</i> , CFU/mL	210000
Particle porosity	0.584	<i>Clostridium</i> , CFU/mL	370000
Total Suspended Solid, mg/L	153950	<i>Staphylococcus sp.</i> , CFU/mL	210000
Volatile Suspended, mg/L	78126	<i>Streptococcus sp.</i> , CFU/mL	490000
Chemical characteristic (dead biomass)		<i>Salmonella sp.</i> , CFU/mL	190000
pH	5.5-6.3	<i>Shiglla dysente</i> , CFU/mL	410000
CEC, meq/100g	51.2	<i>Fungi</i>	
Lead, mg/L	0.02	<i>Penicillium sp.</i> , CFU/mL	180000
Chromium, mg/L	0.01	<i>Yeast</i>	
Cadmium, mg/L	0.02	<i>Candida albicans</i> , CFU/mL	460000
		<i>Protozoa</i>	
		<i>Entamoeba species</i> , CFU/mL	16000
		<i>Giardia lambihia</i> , CFU/mL	90000

(a) Surface area analyzer, BET method, Quantachrome.com.(USA), (b) Apparent density instrument, Autotap, Quantachrome.(USA), CEC Cat ion Exchange Capacity, CFU Colony-forming unit

Procedure

pH of the solutions were adjusted to the desired value (pH=4) using 0.1 M NaOH or 0.1 M HNO₃, with pH higher than 5.5, solubility of metal complexes decreases sufficiently allowing precipitation, which may complicate the sorption process and do not bind to the adsorption sites on the surface of DAB. The flasks were then placed on a shaker (HV-2 ORBTAL, Germany) and agitated continuously for 4 h at 200 rpm and (33±3°C). The samples were filtered by no. 42 Whatman filter paper. Few drops of 0.1 M HNO₃ were added to the samples to decrease the pH below 2 in

order to fix the concentration of the heavy metals during storage before analysis (APHA1995). The final equilibrium concentrations were measured by means of atomic absorption

The fixed bed adsorber was made of an acrylic column of 0.05 m inner diameter and 0.5 m height. DAB bed was confined in the column by fine stainless steel screen and glass cylindrical packing at the bottom and a glass cylindrical packing at the top of the bed to ensure a uniform distribution of influent through the biomass bed. Perforated plate was placed at the top of

the column; the influent solution was introduced to the column through it.

For determination of the biosorption isotherm, different weights (0.05, 0.1, 0.15... to 0.6 g) of dry dead anaerobic biomass were used, (electronic balance Sartorius BL 210S); biosorbents were placed in 12 volumetric flasks of 250 mL. 100 mL of solution with concentration of 50 mg/L was added to each flask for single systems of Pb(II), Cr(III) and Cd(II) ions respectively. The experiment was performed at high metal concentrations so that maximum uptake would be achieved. The adsorbed amount was calculated using the following equation (Sulaymon et al., 2013)

$$q_e = \frac{V_L(C_o - C_e)}{W_A} \quad (19)$$

The necessary dosage of DAB, to reach equilibrium related to the concentration of C_e/C_o equal to 0.05, was calculated from Langmuir isotherm model (eq. 20) and mass balance.

$$q_e = \frac{q_m b C_e}{1 + b C_e} \quad (20)$$

The Langmuir model parameters (q_m and b) were estimated by the nonlinear regression method using STATISTICA version-6 software.

The important characteristic of the Langmuir isotherm can be expressed in terms of the dimensionless constant separation factor for equilibrium parameter (RL). This is defined by

$$RL = \frac{1}{1 + b C_e} \quad (21)$$

The adsorption isotherms were obtained by plotting the weight of solute adsorbed per unit weight of biomass q_e , mg/g against the equilibrium concentration of the solute in the solution C_e , mg/L, and RL eq. (21) (Sulaymon and Ebrahim 2010). The experiments were carried out by using 2 liter pyrex beaker fitted with variable speed mixer. The beaker was filled with 1L of 50 mg/L concentration and the agitation started before adding of DAB. At time zero, the accurate weight of DAB where added and samples were taken at specified time intervals. Pore diffusion coefficient of Pb(II), Cr(III) and Cd(II) was obtained using batch model by matching the concentration decay curve obtained from experimental data. At first time the pore diffusion coefficient is assumed and the

model is solved numerically using MATLAB program. This process continue until obtain perfect matching between the theoretical and experimental concentration decay curve. The results were mentioned in previous paper (Sulaymon et al., 2012). The principle parameter required for solving the batch model is the external mass transfer coefficient and the assumed pore diffusion coefficient. The following steps must be taken to introduce the required parameter conditions

- Estimate the optimum concentration decay curve at optimum agitation speed.
- Numerical solution of the batch model can be used to obtain the theoretical concentration decay curve.
- A good match between the experimental and theoretical concentration decay curves should be obtained.

The external mass transfer coefficient and molecular diffusivity in fixed bed column model were calculated using the correlation of Crittenden (Ahmed, 2006).

$$k_f = 2.4 V_s / (Sc^{0.58} Re^{0.66}) \quad (22)$$

The liquid diffusivity coefficient was calculated using the equation:

$$D_m = 2.74 \times 10^{-9} (MW)^{-1/3} \quad (23)$$

The axial dispersion coefficient of the liquid flowing through fixed beds was obtained from the following correlation (Singh et al, 2012):

$$\frac{D_b}{D_m} = 0.67 + 1.15 \left[\frac{V_s d_p}{D_m} \right]^{1.2} \quad (24)$$

The amount of DAB used for each solute were calculated from final equilibrium related concentration of $C_e/C_o=0.05$ using the Langmuir model with mass balance in 1L of solution. The initial concentration was 50 mg L⁻¹ with the doses of DAB of 1.573, 3.894 and 6.473 g per 1L solution for Pb(II), Cr(III) and Cd(II) ions respectively.

Results and Discussion

Adsorption isotherm

The equilibrium isotherm for the investigated solutes (Pb⁺², Cr⁺³ and Cd⁺²) onto DAB using multi-component Langmuir model are presented in Fig.1 (a,

b and c) respectively. The correlation coefficient (R^2) between the experimental data and the theoretical model is 0.995, 0.990 and 0.985 for lead, chromium and cadmium ions respectively for single biosorption system. The Langmuir parameters are as follows:

- Pb^{+2} : $q_m = 54.92 \text{ mg g}^{-1}$, $b = 0.493 \text{ L mg}^{-1}$, $R^2 = 0.995$
- Cr^{+3} : $q_m = 34.780 \text{ mg g}^{-1}$, $b = 0.107 \text{ L mg}^{-1}$, $R^2 = 0.990$
- Cd^{+2} : $q_m = 29.990 \text{ mg g}^{-1}$, $b = 0.285 \text{ L mg}^{-1}$, $R^2 = 0.985$

While Table 3 shows the experimental results for binary and ternary biosorption batch system

Table 3 shows the experimental results for binary and ternary biosorption batch system

Model	Parameters	Binary system						Ternary system		
		Pb(II)	Cr(III)	Pb(II)	Cd(II)	Cr(III)	Cd(II)	Pb(II)	Cr(III)	Cd(II)
Extended Langmuir $q_i = \frac{b_i q_{m,i} C_{e,i}}{(1 + \sum_{j=1}^n b_j C_{e,j})}$	$q_{m,i} \text{ mg/g}$	35.12	23.84	38.6	11.8	24.51	23.86	15.68	13.86	4.18
	$b_i, \text{ L/mg}$	0.311	0.165	0.142	0.185	0.382	0.039	0.048	0.03	0.09
	R_L	0.084	0.203	0.154	0.314	0.096	0.518	0.571	0.706	0.727
	R^2	0.958	0.999	0.996	0.992	0.993	0.999	0.995	0.986	0.992

Pore diffusion coefficient

Pore diffusion coefficients of lead, chromium and cadmium ions were obtained using batch model by matching the concentration decay curve obtained from experimental data at optimum agitation speed 400 rpm with that obtained from the batch model as shown in Fig. 2.

The pore diffusion coefficient for each solute is evaluated from batch experiments to be:

- Pb^{+2} : $D_p = 7.23 \times 10^{-11} \text{ m}^2 \text{ s}^{-1}$, $R^2 = 0.994$
- Cr^{+3} : $D_p = 3.15 \times 10^{-11} \text{ m}^2 \text{ s}^{-1}$, $R^2 = 0.995$
- Cd^{+2} : $D_p = 2.76 \times 10^{-11} \text{ m}^2 \text{ s}^{-1}$, $R^2 = 0.98$

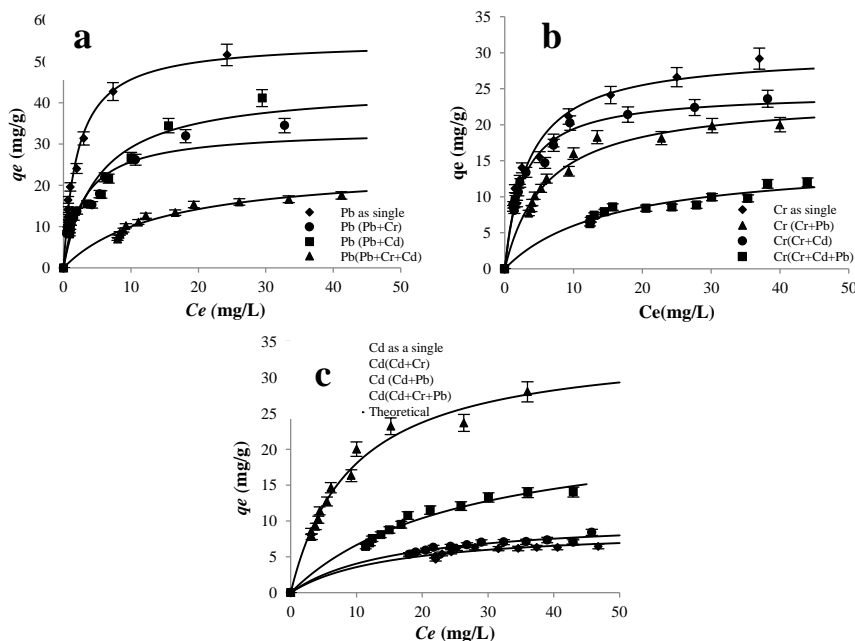


Fig. 1 (a, b, and c) Biosorption isotherms for lead, chromium and cadmium ions onto DAB, in single, binary and ternary systems $C_0=50 \text{ mg/l}$ respectively

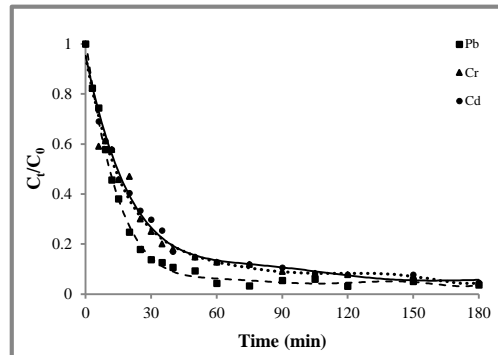


Fig. 2. Comparison of the measured concentration-time decay data with that predicted by pore diffusion model for Pb^{+2} , Cr^{+3} and Cd^{+2} .

The adsorption capacity order for lead, chromium and cadmium onto DAB was as follow:

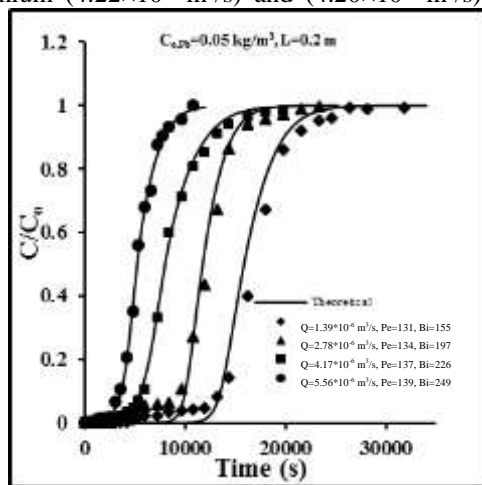
Pb^{+2} (54.92 mg g^{-1}) > Cr^{+3} (34.78 mg g^{-1}) > Cd^{+2} (29.99 mg g^{-1}). This behavior of the capacity of the adsorbate in single batch system seems to influence the adsorption capacity of DAB in fixed bed adsorber. This can be explained by:

- a- Lead has less solubility (520000 mg L^{-1}) in water compared with chromium and cadmium (810000 mg L^{-1}) and ($1360000 \text{ mg L}^{-1}$) respectively.
- b- Lead has higher molecular diffusion ($4.98 \times 10^{-8} \text{ m}^2/\text{s}$) in water compared with chromium and cadmium ($4.22 \times 10^{-8} \text{ m}^2/\text{s}$) and ($4.20 \times 10^{-8} \text{ m}^2/\text{s}$)

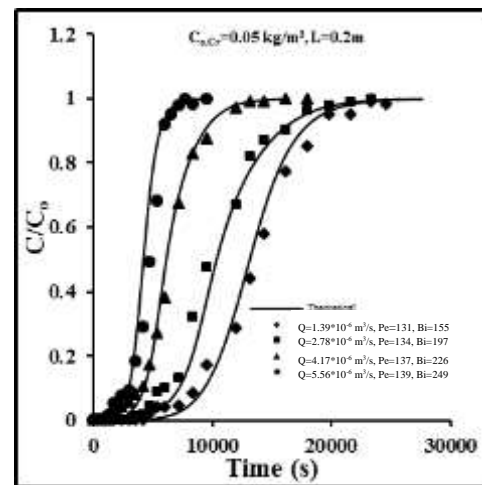
respectively, which can be adsorbed by means of electrostatic attraction between positively charged and negatively charged binding sites. (Physical adsorption by means of Van der Waals).

Breakthrough curves of the single, binary and ternary systems:

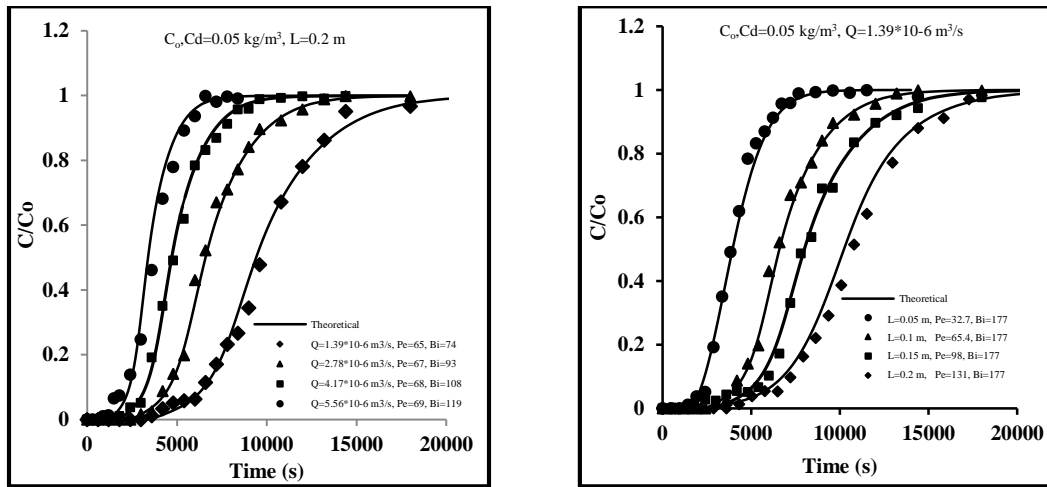
The experimental and predicted breakthrough curves for single binary and ternary systems for adsorption of lead, chromium and cadmium onto DAB at different flow rate, bed height and initial concentration are shown in Figs. 3, 4 and 5 (a, b, c and d) respectively, while Table 4 shows Biot and Peclet number



(a) Experimental and predicted breakthrough curves for single biosorption of lead onto DAB at different flow rate



(b) Experimental and predicted breakthrough curves for single biosorption of chromium onto DAB at different flow rate.



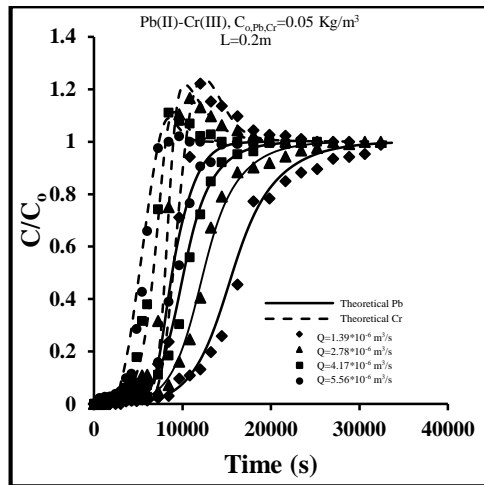
(c) Experimental and predicted breakthrough curves for single biosorption of cadmium onto DAB at different flow rate

(d) Experimental and predicted breakthrough curves for single biosorption of cadmium onto DAB at different bed height.

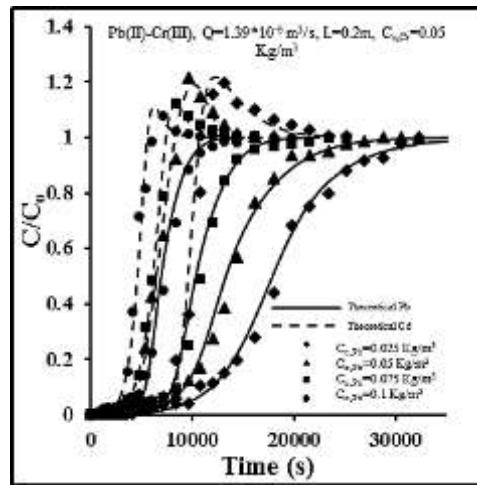
Fig. 3 Experimental and predicted breakthrough curves for single biosorption of lead, chromium and cadmium onto DAB at different flow rates and bed heights

Table 4 The values of Biot no. and Peclet no. at different flow rates and bed heights.

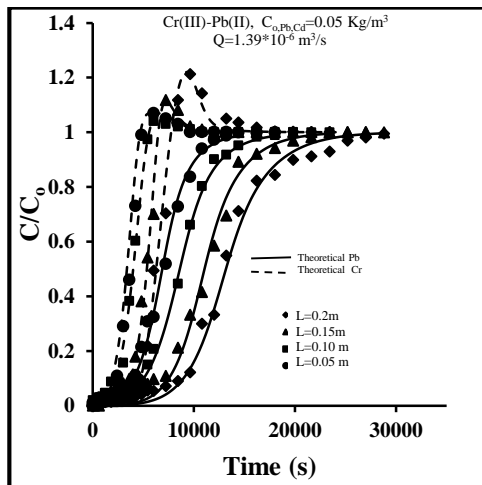
Pollutants	Flow rate, m ³ s ⁻¹	Biot no. (Bi)	Peclet no. (Pe)	Bed height, m	Biot no. (Bi)	Peclet no. (Pe)
Pb ⁺²	1.39×10 ⁻⁶	74.6	131	0.05	74.6	32.7
	2.78×10 ⁻⁶	93.3	134	0.10	74.6	65.4
	4.17×10 ⁻⁶	108	137	0.15	74.6	98.0
	5.56×10 ⁻⁶	119	139	0.20	74.6	131.0
Cr ⁺³	1.39×10 ⁻⁶	115	131	0.05	155	32.7
	2.78×10 ⁻⁶	197	134	0.10	155	65.4
	4.17×10 ⁻⁶	226	137	0.15	155	98.0
	5.56×10 ⁻⁶	249	139	0.20	155	131.0
Cd ⁺²	1.39×10 ⁻⁶	177	131	0.05	177	32.7
	2.78×10 ⁻⁶	224	134	0.10	177	65.4
	4.17×10 ⁻⁶	257	137	0.15	177	98.0
	5.56×10 ⁻⁶	283	139	0.20	177	131.0



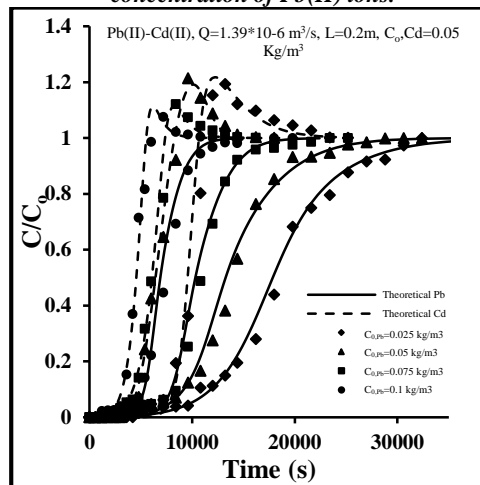
(a) Experimental and predicted breakthrough curves for binary biosorption of Pb(II)-Cr(III) system onto DAB at different flow rate



(b) Experimental and predicted breakthrough curves for binary biosorption of Pb(II)-Cd(II) system onto DAB at different initial concentration of Pb(II) ions.

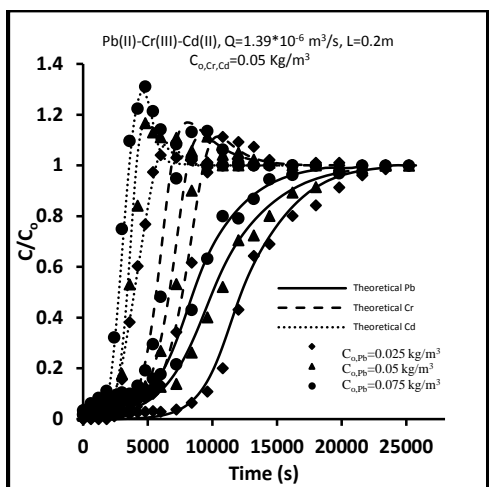


(c) Experimental and predicted breakthrough curves for binary biosorption of Cr(III)-Pb(II) system onto DAB at different bed height

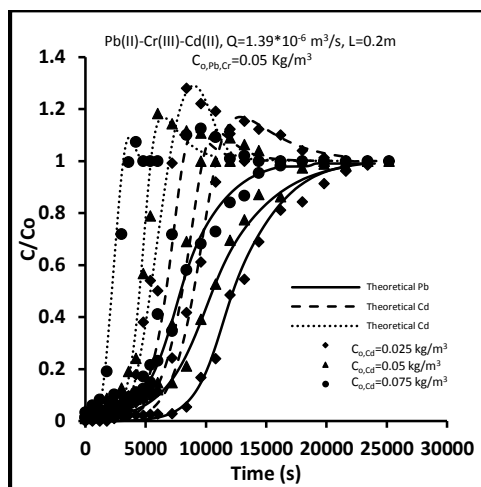


(d) Experimental and predicted breakthrough curves for binary biosorption of Pb(II)-Cd(II) system onto DAB at different initial concentration of Pb(II) ions.

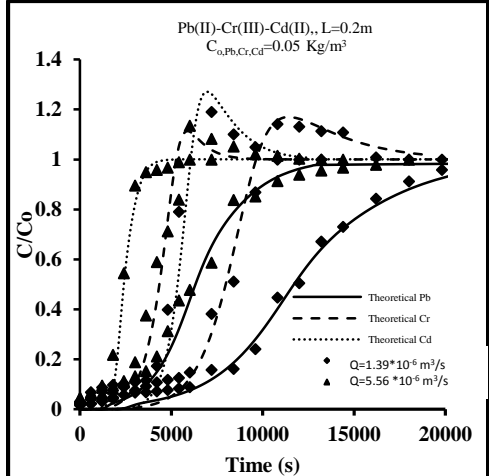
Fig. 4 Experimental and predicted breakthrough curves for binary biosorption system of lead, chromium and cadmium onto DAB at different flow rates and bed heights



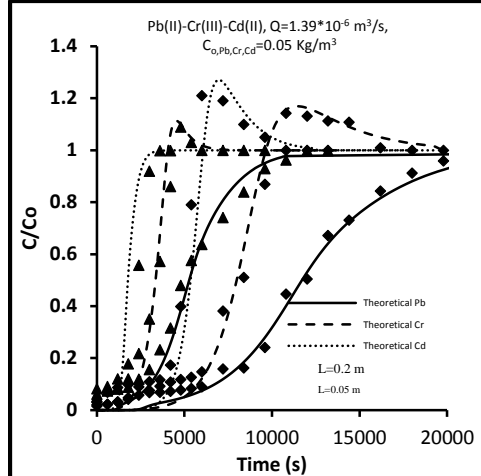
(a) Experimental and predicted breakthrough curves for ternary biosorption of Pb(II)-Cr(III)-Cd(II) system onto DAB at different Pb(II) initial concentration.



(b) Experimental and predicted breakthrough curves for ternary biosorption of Pb(II)-Cr(III)-Cd(II) system onto DAB at different Cd(II) initial concentration



(c) Experimental and predicted breakthrough curves for ternary biosorption of Pb(II)-Cr(III)-Cd(II) system onto DAB at different flow rate



(d) Experimental and predicted breakthrough curves for ternary biosorption of Pb(II)-Cr(III)-Cd(II) system onto DAB at different bed height

Fig. 5 Experimental and predicted breakthrough curves for ternary biosorption system of lead, chromium and cadmium onto DAB at different flow rates and bed heights

Effect of flow rate: Figs (3, 4 and 5) show the experimental and predicted breakthrough curves for Pb^{+2} , Cr^{+3} and Cd^{+2} in single, binary and ternary systems at different flow rates (1.39×10^{-6} , 2.78×10^{-6} and $4.17 \times 10^{-6} \text{ m}^3 \text{ s}^{-1}$) in terms of C/C_0 . It's clear from these figures that as the flow rate increases, the time of breakthrough point decreases. This is because the residence time of solute in the bed decreases. Therefore there is not enough time for adsorption equilibrium to be reached which results in lower bed

utilization and the adsorbate solution leaves the column before equilibrium. It is expected that the change in flow rate will affect the film diffusion but not the intra-particle diffusion. The higher the flow rates, the smaller film resistance to mass transfer and hence larger k_f results. Increasing flow rate at constant bed height will increase the Bi number with slight increase in Pe number as listed in Table 4. When the Bi number is high the time of breakthrough point will appear early. The higher Bi number values indicate

that the film diffusion is not dominating compared to the intra-particle mass transfer and the intra-particle mass transfer is the controlling step. These results agree with those obtained by Sulaymon et al.,(2012)

Effects of bed height: the bed height is one of the major parameters in the design of fixed bed adsorption column (Rao et al., 2011). The experimental and predicted breakthrough curves obtained for different heights of DAB 0.05, 0.1, 0.15 and 0.2 m at constant flow rate and constant initial concentration are presented in the above figures. It is clear that, at smaller bed height the C_e/C_o increase more rapidly than at higher bed height. Furthermore, at smaller bed height the bed is saturated in less time compared with the deeper bed height. Increasing the bed height at constant flow rate increases Pe numbers as listed in Table 4. When Pe number is small, the break point appears early and increases with the Pe number. Hence, the internal and external resistances are confirmed to be the main parameters that control the adsorption kinetics with the increase in bed height. It is clear that increasing bed height increases the breakthrough time and the residence time of the lead, chromium and cadmium solution in the bed, since the bed volume of DAB increased. Similar findings have been obtained by Sulaymon et al., (2009).

Effect of initial concentration: The change in initial concentration of lead, chromium and cadmium will have a significant effect on the breakthrough curves. The experimental and predicted breakthrough curves obtained at different initial concentration (25, 50, 75

and 100 mg L⁻¹). As the initial concentration increases the time of breakthrough point decreases. The higher the initial concentration, the faster the breakthrough curves; however, the DAB loadings are higher at higher initial concentration. For high initial concentration, steeper breakthrough curves are found because the equilibrium is attained faster. These results are in agreement with that obtained by Aksu and Gonen, (2004)

In multi-component system (binary and ternary system) for lead, chromium and cadmium, at the initial stage, there are a lot of active sites of DAB, and the strongly (Pb⁺²) and weakly (Cd⁺²) adsorbed component take the active site freely. With increasing time, the weakly adsorbed component is not easily adsorbed but moves ahead with the bulk-fluid and the strongly adsorbed component tends to displace the sites that had been taken by the weakly adsorbed component. The result is that the local concentration of the weakly adsorbed component within the fixed bed adsorber is higher.

From the above results it is clearly that the simulated breakthrough curves for adsorption lead, chromium and cadmium ions in single, binary and ternary systems onto DAB are in close agreement with the experimental results. Thus, the mathematical model, which includes axial dispersion, film mass transfer, pore diffusion resistance and nonlinear isotherm, provides a good description of the single and competitive adsorption process in fixed bed adsorber.

Nomenclature

Å	Angstrom, 1×10^{-10} m
b	Adsorption equilibrium constant relate to affinity between adsorbent and adsorbate, L mg ⁻¹
Bi	Biot number
C	Fluid phase concentration, mg L ⁻¹
C _e	Equilibrium liquid phase concentration, mg L ⁻¹
C _o	Initial liquid phase concentration, mg L ⁻¹
D _b	Axial dispersion coefficient m s ⁻¹
D _m	Molecular diffusivity, m ² s ⁻¹
D _p	Pore diffusion coefficient, m ² s ⁻¹
d _p	Particle diameter, m
k _f	External mass transfer coefficient, m s ⁻¹
MW	Molecular weight, g mol ⁻¹
L	Length of the column, m
P _e	Peclet number
Q	Flow rate, m ³ s ⁻¹
q _e	Adsorption capacity at equilibrium, mg g ⁻¹
q _m	Langmuir constant related to maximum adsorption capacity, mg g ⁻¹

r	Radial coordinate, m
R	Radial coordinate, m
Re	Renold number, $Re = \rho_w v d_p / \mu_w$
R_p	Radius of particle, m
Sc	Schmidt number, $Sc = \mu_w / \rho_w D_m$
Sh	Sherwood number, $Sh = k_r d_p / D_m$
t	Time, s
V_L	Volume of solution, L
W_A	Mass of DAB, g
Z	Axial distance, m
ϵ_b	Bed porosity
ϵ_p	Particle porosity
μ_w	Viscosity of water $N\ s\ m^{-2}$
v	Interstitial velocity, $v = Q / \pi R^2 \epsilon_b$
ρ_w	Density of water, $kg\ m^{-3}$
ρ_p	Particle density, $kg\ m^{-3}$
Subscript	
b	Bulk fluid phase
e	equilibrium
DAB	Dead anaerobic biomass
i	Component number, 1,2,...
L	Liquid Phase
o	Initial phase
p	Particle phase

References

- Ahmed KW (2006) Removal of multi-pollutants from wastewater by adsorption method, Ph.D. Thesis, University of Baghdad, Iraq
- Aksu Z, Gonen F (2004) Biosorption of phenol by immobilized activated sludge in a continuous packed bed: prediction of breakthrough curves. *Process.Biochem.* 39: 599–613
- Alkhalifa AH, Al-Homaidan AA, Shehata AI, Al-Khamis HH, Al-Ghanayem AA and Ibrahim AS. (2012) Brown macroalgae as bio-indicators for heavy metals pollution of Al-Jubail coastal area of Saudi Arabia. *African Journal of Biotechnology* 11(92): 15888-15895
- Al-Najar JA (2009) Removal of heavy metals by adsorption using activated carbon and Kaolinite, Ph.D Thesis, University of Technology, Baghdad, Baghdad, Iraq
- Gupta VK, Rastogi A (2009) Biosorption of hexavalent chromium by raw and acid-treated green alga *Oedogonium hatei* from aqueous solutions. *J Hazard Mater* 163:396 – 402
- Hawari HA, Mulligan NC (2006) Biosorption of lead (II), copper (II), and nickel (II) by anaerobic granular biomass. *Bioresour Technol* 97:692 –700
- Jianlong W, Can C (2009) Biosorbents for heavy metals removal and their future. *Biotechnol Adv* 27:195– 226
- Lawrence K, Wang JT, Stephen TT, Yung-Tse H (2010) Handbook of environmental engineering, environmental bioengineering. Springer, New York
- Rao KS, Anand S, Venkateswarlu P(2011) Modeling the kinetics of Cd(II) adsorption on *Syzygium cumini* L leaf powder in a fixed bed mini column. *J.Ind. Eng. Chem.* 17L: 174–181
- Singh A, Kumar D, Gaur JP (2012) Continuous metal removal from solution and industrial effluents using *Spirogyra* biomass-

- packed column reactor, Water Research,46 (3), 779-788
11. Sulaymon AH, Abbood DW, Ali AH (2012) Removal of phenol and lead from synthetic wastewater by adsorption onto granular activated carbon in fixed bed adsorbers: prediction of breakthrough curves Desalination and Water Treatment 40(1-3): 244-253
 12. Sulaymon AH, Ebrahim SE (2010) Removal of lead, cadmium, and mercury ions using biosorption. Desalin Water Treat 24:344 – 35
 13. Sulaymon AH, Ebrahim SE and Mohammed-Ridha MJ (2013) Equilibrium, kinetic, and thermodynamic biosorption of Pb(II), Cr(III), and Cd(II) ions by dead anaerobic biomass from synthetic wastewater. Environ Sci Pollut Res 20:175-187
 14. Vijayaraghavan K, Yun Y-S (2008) Bacterial biosorbents and biosorption. Biotechnol Adv 26:266 – 291
 15. Volesky B, May H, Holan ZR (2004) Cadmium biosorption by *Sac-charomyces cerevisiae* . Biotechnol Bioeng 41:826 –829